Performance Analysis of Conventional STATCOMs and STATCOMs with Energy Storage in Electric Arc Furnace Applications

Antti Virtanen, Heikki Tuusa
Tampere University of Technology
Department of Electrical Energy Engineering
Tampere, Finland
Email: antti.a.virtanen@tut.fi

Jarmo Aho
Alstom Grid
Tampere, Finland
Email: jarmo.aho@alstom.com

***Abstract*—This paper analyzes the performance and power losses of 2.1 MVA conventional STATCOMs and STATCOMs with energy storage (ESTATCOM), in electric arc furnace applications. The research was conducted by computer simulations with Matlab Simulink software. According to the simulation results load compensation reduces the required current rating of the supply grid transformer and cables by approximately 30 %, and the maximum drop of the reference point (RP) voltage to 2 % compared to 15 % caused by the non-compensated case. The conventional STATCOM attenuates the RP voltage flicker by a factor of 5.9 and the ESTATCOM by a factor of 11.7. The voltage source converters (VSC) of both compensators could be designed for the same rated current, despite the active power compensation capabilities of the ESTATCOM. The system losses are minimized when a 3-level VSC is used instead of a 2-level VSC, and the compensating device is connected to the lowest studied network voltage of 690 V. The energy storage system losses are minimized when the energy storage is connected to the dc link using two separate DC/DC converters instead of a large single converter. This occurs because the system converters can be implemented with IGBTs of lowest rated voltage.**

I. INTRODUCTION

Static synchronous compensators (STATCOM) are power electronic devices used to compensate e.g. voltage sags, voltage flicker, voltage unbalances and harmonics in power systems [1–5]. A conventional STATCOM is capable of regulating the power system voltage by exchanging reactive power with the network. The integration of energy storage (ES) enables the device to exchange also active power with the network (ESTATCOM), which is beneficial in cases where power quality problems are caused by the fluctuating active power, especially in weak networks [6], [7].

This paper presents a performance analysis of 2.1 MVA conventional STATCOMs and ESTATCOMs in electric arc furnace (EAF) applications. The systems are compared in terms of supply current compensation capabilities, reference point (RP) voltage amplitude and flicker compensation properties, likewise the required current ratings of the compensator voltage source converters (VSC). In addition, the influence of the network voltage level, VSC topology, and ES integration on the system losses is analyzed. The research was performed using computer simulations with Matlab Simulink software.

Section II presents an overview of the non-compensated (NC) EAF system, as well as the compensator configurations studied and their control systems. Section III presents the criteria used for analyzing the system performances, and the simulation results. Finally, conclusions are drawn in Section IV.

II. SYSTEMS STUDIED

A. The Non-Compensated EAF System

A typical EAF installation is presented in Fig. 1a. The nominal power of the EAF is 100 MVA. It is connected to a 33 kV distribution feeder with the transformer T_{EAF}, which has the short circuit power of 1000 MVA with an impedance X/R-ratio of 5.4. When high rapidly varying and unbalanced currents are drawn through the system impedances Z_1 and Z_2 the voltage at the point of common coupling (PCC) experiences heavy fluctuation, hence a compensator such as a STATCOM is connected to the RP in parallel with the load.

In 100 MVA-class applications the compensation system consists of several smaller compensation units connected to the RP. This study focuses only on the operation of a single compensation unit with nominal power of 2.1 MVA. This leads to the reduced system presented in Fig. 1b, in which the nominal power of the EAF has also been reduced to 2.1 MVA. In addition, the 220 kV transfer network of Fig. 1a has been assumed to be stiff, i.e. $Z_1 = 0$. The supply grid short-circuit power is 21 MVA, and the systems were studied with grid line-to-line voltages of 2 kV, 1 kV and 690 V. The grid inductances L_{grid} and resistances R_{grid} are presented in Table I.

978-1-4673-4355-8/13/$31.00 ©2013 IEEE

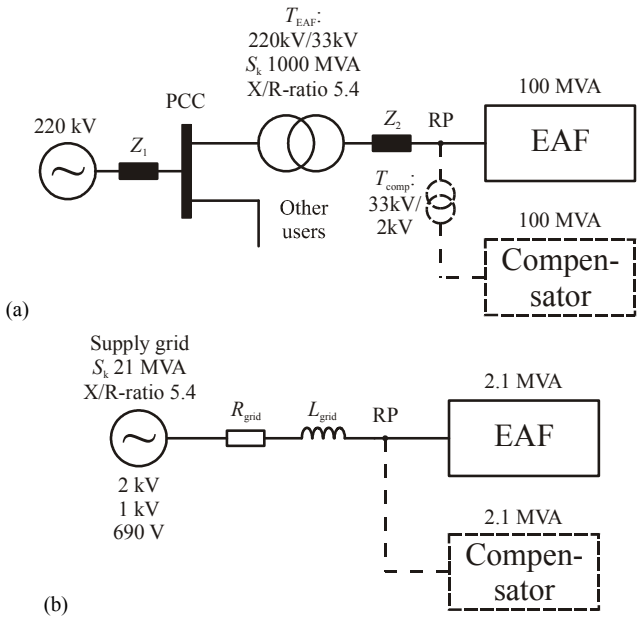

Figure 1. (a) Typical EAF installation, (b) reduced arrangement.

B. Compensator Configurations

Figs. 2 and 3 present an overall picture of the compensator configurations studied and their control systems. The conventional STATCOMs consist of a shunt-connected VSC, an LCL-filter, and dc link capacitors C_{dc}. These can be upgraded to ESTATCOMs by connecting an ES to the system dc link. The ESs are connected to the dc link with either a single 1.1 MW bidirectional DC/DC converter, or with two separate 0.55 MW converters as presented with the dashed line in Fig. 3. The system dc link voltages u_{dc} are 3500 V, 1750 V and 1200 V.

The ESs are supercapacitor (SC) banks built-up of case-specific series- and parallel connections of Maxwell BMOD0063 P125 modules for a maximum continuous total power of 1.1 MW with maximum continuous current of 150 A for a single module. The SC bank configurations are presented in Table II [8], [9].

The VSC bridge topologies are either 3-phase 2-level converters or 3-level neutral point clamped (NPC) converters [10], [11], and the topology of the DC/DC converters is 3-phase step-up/step-down with 120° interleaved PWM modulation [12]. In this study the PWM modulators of the converters were excluded, hence the converters execute their voltage and current references $u^*_{VSC,abc}$ and i^*_{SC} ideally. Instead, in order to simulate the system power losses and lighten the computational burden, power loss models for the converter bridges, LCL-filters, DC/DC converter chokes, and SC banks, presented in [9], were used.

TABLE I. SUPPLY GRID INDUCTANCES AND RESISTANCES

Supply voltage	Inductance L_{grid} [mh (p.u.)]	Resistance R_{grid} [mΩ (p.u.)]
2 kV	0.6 (0.1)	35 (0.02)
1 kV	0.15 (0.1)	8.8 (0.02)
690 V	0.07 (0.1)	4.2 (0.02)

TABLE II. SUPERCAPACITOR BANKS OF THE ESTATCOM CONFIGURATIONS

System	Modules in series	Series connections in parallel
1.1 MW 2 kV	20	3
2×0.55 MW 2 kV	10	3×2
1.1 MW 1 kV	10	6
2×0.55 MW 1 kV	5	6×2
1.1 MW 690 V	7	8
2×0.55 MW 690 V	4	8×2

Table III presents the passive elements of the systems studied. Each LCL-filter was designed for maximum compensator current i_{comp} THD of 2 %, and for maximum $i_{comp,rms}$ switching frequency ripple of 2 %. The resonance frequency of each filter is 1620 Hz. The DC/DC converter inductors $L_{dc/dc}$ were designed for a maximum peak-to-peak current ripple of 10 % in the SC current i_{SC}. The SC bank capacitances C_{SC} and the equivalent series resistances $R_{ESR,SC}$ were calculated on the basis of single module parameters C_{SC} = 63 F and $R_{ESR,SC}$ = 18 mΩ, found in the manufacturer's datasheet and in [8], [9].

C. Compensator Control Systems

The control systems of both compensators were implemented in the reference frame synchronized to the positive sequence component of the RP voltage vector $\underline{u}_{RP}$.

TABLE III. COMPONENTS OF THE SYSTEMS STUDIED

System	L_{f1} [mH (p.u.)]	L_{f2} [mH (p.u.)]	C_f [mF (p.u.)]	R_{damp} [Ω (p.u.)]	C_{dc} [mF (p.u.)]	$L_{dc/dc}$ [mH (p.u.)]	C_{SC} [F (p.u.)]	$R_{ESR,SC}$ [mΩ (p.u.)]
3-Level 2kV / 2×DCDC	0.1 (0.016)	0.4 (0.063)	0.12 (0.075)	1.33 (0.67)	4.8 (3.0)	1.6 (0.25) / 2×0.8 (0.125)	9.45 (5900) / 2×18.9 (11800)	120 (0.06) / 2×60 (0.03)
3-Level 1kV / 2×DCDC	0.025 (0.016)	0.1 (0.063)	0.48 (0.075)	0.33 (0.67)	19.2 (3.0)	0.4 (0.25) / 2×0.2 (0.125)	37.8 (5900) / 2×75.6 (11800)	30 (0.06) / 2×15 (0.03)
3-Level 690V / 2×DCDC	0.0125 (0.017)	0.05 (0.066)	0.96 (0.072)	0.17 (0.70)	40.3 (3.0)	0.21 (0.27) / 2×0.105 (0.135)	72.0 (5360) / 2×126 (9380)	16 (0.07) / 2×9 (0.04)
2-Level 2kV / 2×DCDC	0.2 (0.032)	0.8 (0.126)	0.06 (0.037)	2.66 (1.33)	4.8 (3.0)	1.6 (0.25) / 2×0.8 (0.125)	9.45 (5900) / 2×18.9 (11800)	120 (0.06) / 2×60 (0.03)
2-Level 1kV/ 2×DCDC	0.05 (0.032)	0.2 (0.126)	0.24 (0.037)	0.67 (1.33)	19.2 (3.0)	0.4 (0.25) / 2×0.2 (0.125)	37.8 (5900) / 2×75.6 (11800)	30 (0.06) / 2×15 (0.03)
2-Level 690V / 2×DCDC	0.025 (0.033)	0.1 (0.132)	0.48 (0.036)	0.33 (1.4)	40.3 (3.0)	0.21 (0.27) / 2×0.105 (0.135)	72.0 (5360) / 2×126 (9380)	16 (0.07) / 2×9 (0.04)

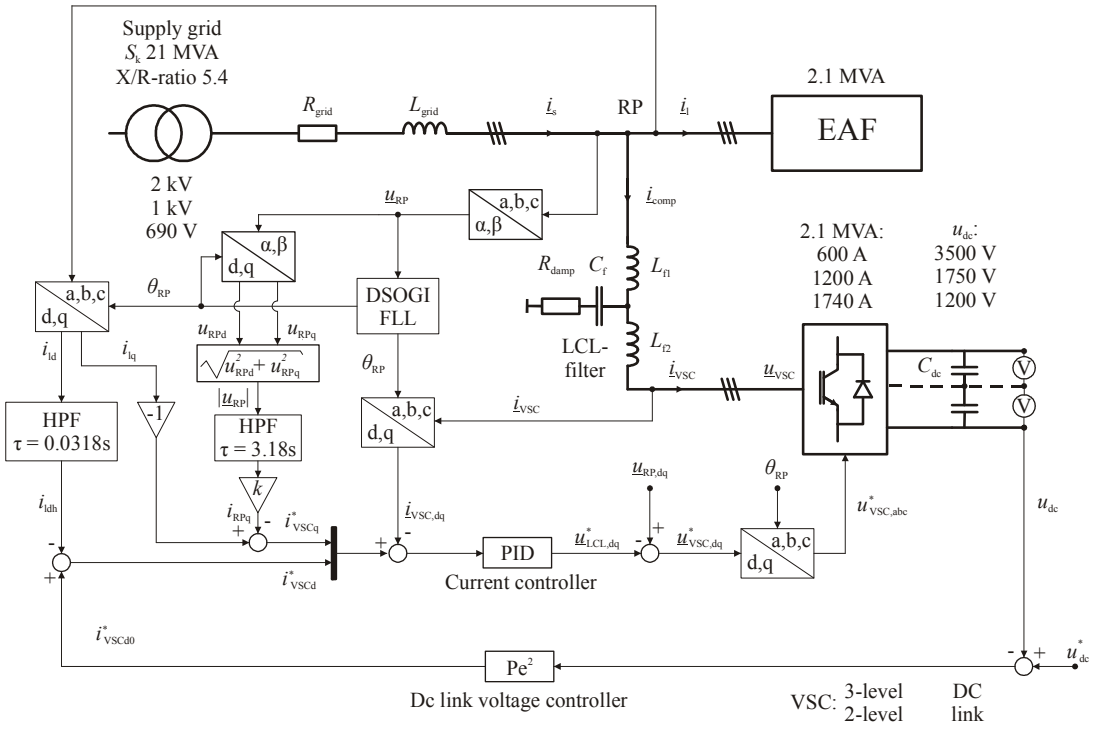

Figure 2. Conventional STATCOM configurations and control system.

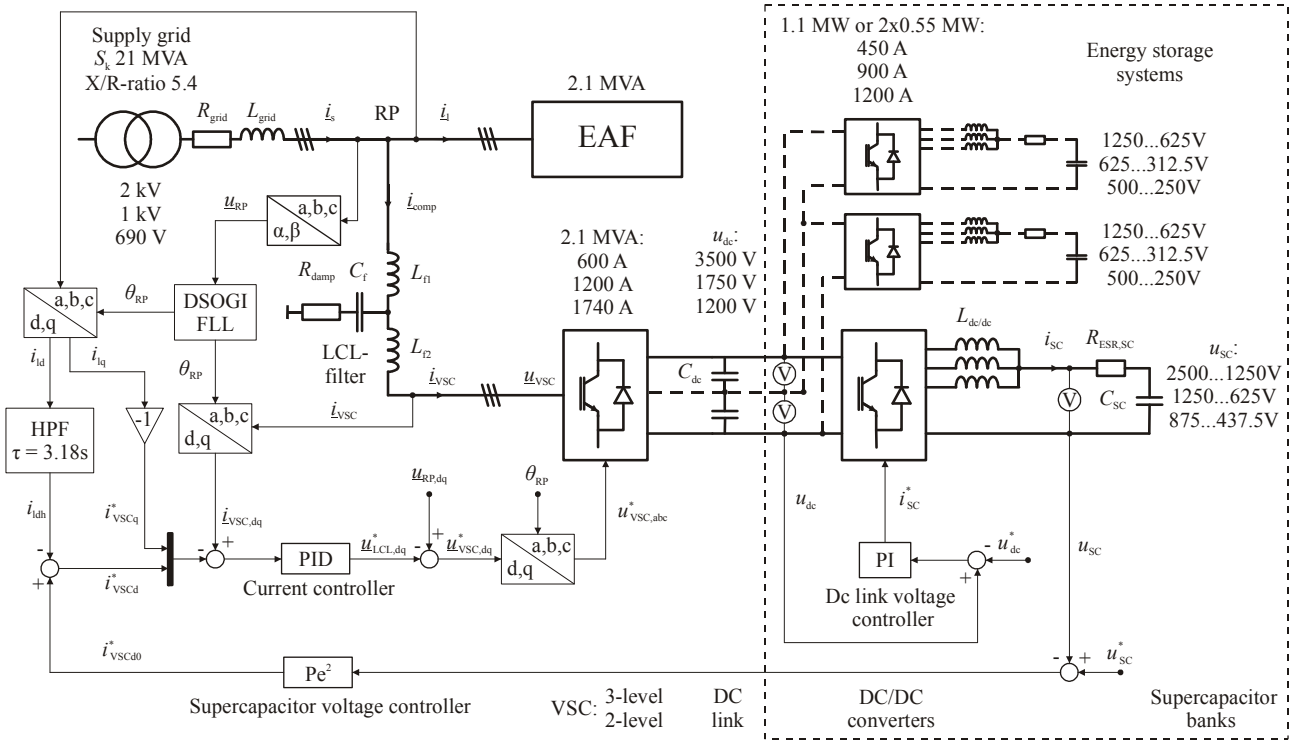

Figure 3. ESTATCOM configurations and control system.

Because EAFs are heavy loads that draw rapidly changing unbalanced currents from the grid, the grid synchronization was carried out with the DSOGI-FLL, which has been proven to be a precise and fast method for tracking the $\underline{u}_{RP}$ angle θ_{RP} under unbalanced grid conditions [13], [14].

The control system of the conventional STATCOM (Fig. 2) consists of three parts. The first part compensates the load current imaginary component i_{lq} to zero, which would lead to zero imaginary power in the RP if this was the only control objective. The second part consists of an open-loop RP voltage controller, which outputs an imaginary current component i_{RPq} after high-pass filtering (HPF) the measured $|\underline{u}_{RP}|$. With positive i_{RPq} imaginary power is injected into the grid, and the u_{RP} increases. With negative i_{RPq} imaginary power is drawn from the grid, and the u_{RP} decreases. The time constant of the RP voltage controller HPF is $\tau = 3.18$ s and the gain $k = 1$. The third part compensates the harmonics in the supply current $\underline{i}_s$ by high-pass filtering the load current real component i_{ld} with a first order HPF with a time constant of $\tau = 0.0318$ s. In addition the system includes a dc link voltage controller designed to maintain u_{dc} around its reference u^*_{dc}, by producing the reference i^*_{VSCd0}. Finally the VSC current references i^*_{VSCd} and i^*_{VSCq} are transferred to the current control loop, which produces the VSC reference voltages $u^*_{VSC,abc}$.

The objective of control for the ESTATCOM is to compensate i_{sd} to the average level of i_{ld}, and to compensate i_{sq} to zero. Thus, steady average active power is drawn from the grid, and the RP imaginary power becomes fully compensated. This is achieved by high pass filtering the i_{ld} with a first order HPF with time constant $\tau = 3.18$ s, inverting the i_{lq}, and by transferring the obtained references i^*_{VSCd} and i^*_{VSCq} to the current control loop. The DC/DC converter control system maintains the dc link voltage u_{dc} around its reference u^*_{dc}, and the SC voltage control system maintains the SC voltage u_{SC} within its desired operating range under long-term operation.

III. Simulation Results

The following indicators were used for analyzing the performances of the systems studied:

1) Supply transformer and cable current ratings

2) RP voltage regulation and flicker indices

3) Compensator VSC current ratings

4) Total energy consumption

The systems were simulated with an EAF load cycle of 6 s. Figs. 4a–h present the simulated waveforms for the compensated systems using 3-level VSCs with network voltage of 2 kV, and also for the non-compensated (NC) system. In the figures the ESTATCOM waveforms are presented in red, the conventional STATCOM in green, and the NC system in blue. Figs. 5a,b present a comparison of the total energy consumptions and efficiencies for all systems studied. A summary of the performance indicators is presented in Table IV, in which the percentual values apply to all systems also with the voltage levels of 1 kV and 690 V.

The RP active- and imaginary powers of Figs. 4a,b indicate that the ESTATCOM is capable of compensating both the RP imaginary power to zero, and the active power to the average level of the load, as discussed in Section II.C. The conventional STATCOM imaginary power at the RP differs slightly from the ESTATCOM, because of the u_{RP} control system which injects or absorbs imaginary power depending on the fluctuating u_{RP}. In addition the u_{dc} control utilizes grid active power and, hence the RP active power fluctuates more than with the ESTATCOM. Figs. 4c–f present the d- and q-components of $\underline{i}_s$ and $\underline{u}_{RP}$, as well as their zoomed 3-phase waveforms for 100 ms. The heavy unbalance in the EAF currents is clearly visible in the 3-phase waveforms in the NC system. The ESTATCOM compensates both the amplitude variations and the unbalance in the currents, while some disturbances still persist in the conventional STATCOM currents. The RMS values of the supply currents over the 6 s load cycle, presented in Table IV, indicate that load compensation could reduce the required current rating of the supply grid cable and transformer by approximately 30 % compared to the NC system.

The maximum RP voltage drops are significantly reduced due to compensation from approximately 15 % to around 2 % depending on the compensator device (Table IV). The voltage flicker indices P_{st} of the u_{RP} were analyzed with a flicker meter simulation model implemented in accordance with the standard IEC-61000-4-15 [15]. The best flicker attenuation of 11.7 was achieved with the ESTATCOM, which is capable of compensating the flicker very close to the threshold level for irritating voltage flicker of $P_{st} = 1.0$ p.u. An attenuation of 5.9 is achieved with the conventional STATCOM, but the flicker index is about twice as high ($P_{st} = 2.07$) when compared to the ESTATCOM.

The currents of the compensator VSCs, presented in Fig. 4g and Table IV, indicate that the RMS- and peak values of both compensator currents are approximately equal to each other. Thus the active power compensation does not significantly increase the currents through the ESTATCOM IGBTs in comparison with the conventional STATCOM.

Fig. 4h presents the ESTATCOM SC bank voltage u_{SC} and the individual module current. The u_{SC} fluctuates around its reference (2400 V) depending on whether active power is injected or absorbed from the grid. The SC module current is maintained below the maximum continuous rating of 150 A.

TABLE IV. Summary of Performance Indicators

Phase-a supply current RMS (A / % of NC)	
NC	398.0 A / 100 %
STATCOM	278.0 A / 69.8 %
ESTATCOM	272.5 A / 68.5 %
Min. RP line-to-line voltage (V / % drop of U_N (2 kV))	
NC	1710 V / 14.5 %
STATCOM	1962 V / 1.9 %
ESTATCOM	1973 V / 1.4 %
RP voltage flicker indices (P_{st} / attenuation)	
NC	12.21 / 1.00
STATCOM	2.07 / 5.9
ESTATCOM	1.04 / 11.7
VSC currents (Arms / Apeak / % of i_{max} (1200 A))	
STATCOM	225.3 A / 1106 A / 92.2 %
ESTATCOM	228.3 A / 1096 A / 91.3 %

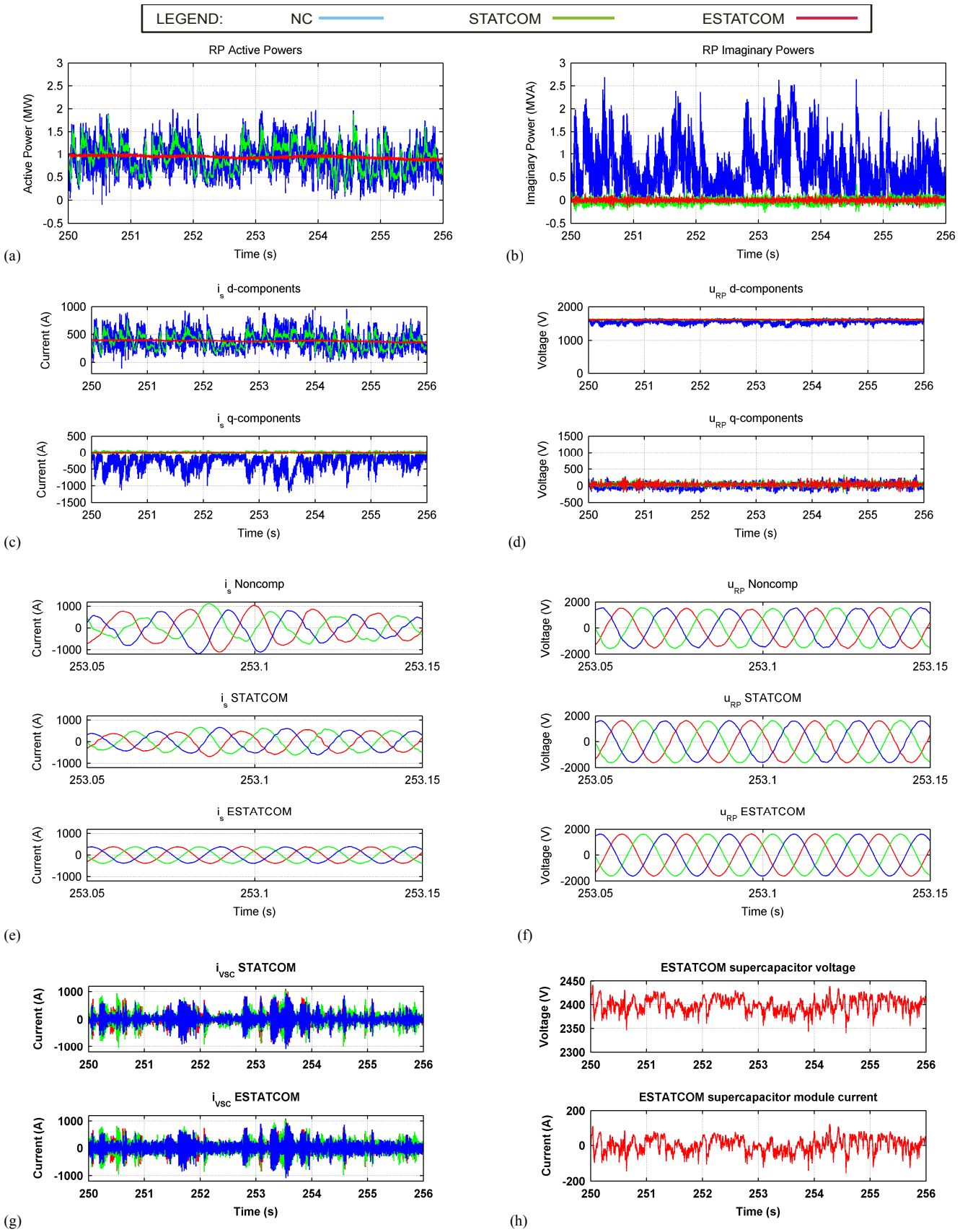

Figure 4. Simulation results. (a) RP active powers, (b) RP imaginary powers, (c) Supply current dq-components, (d) RP voltage dq-components, (e) supply 3-phase currents zoomed, (f) RP 3-phase voltages zoomed, (g) compensator VSC phase currents, and (h) SC voltage and module current.

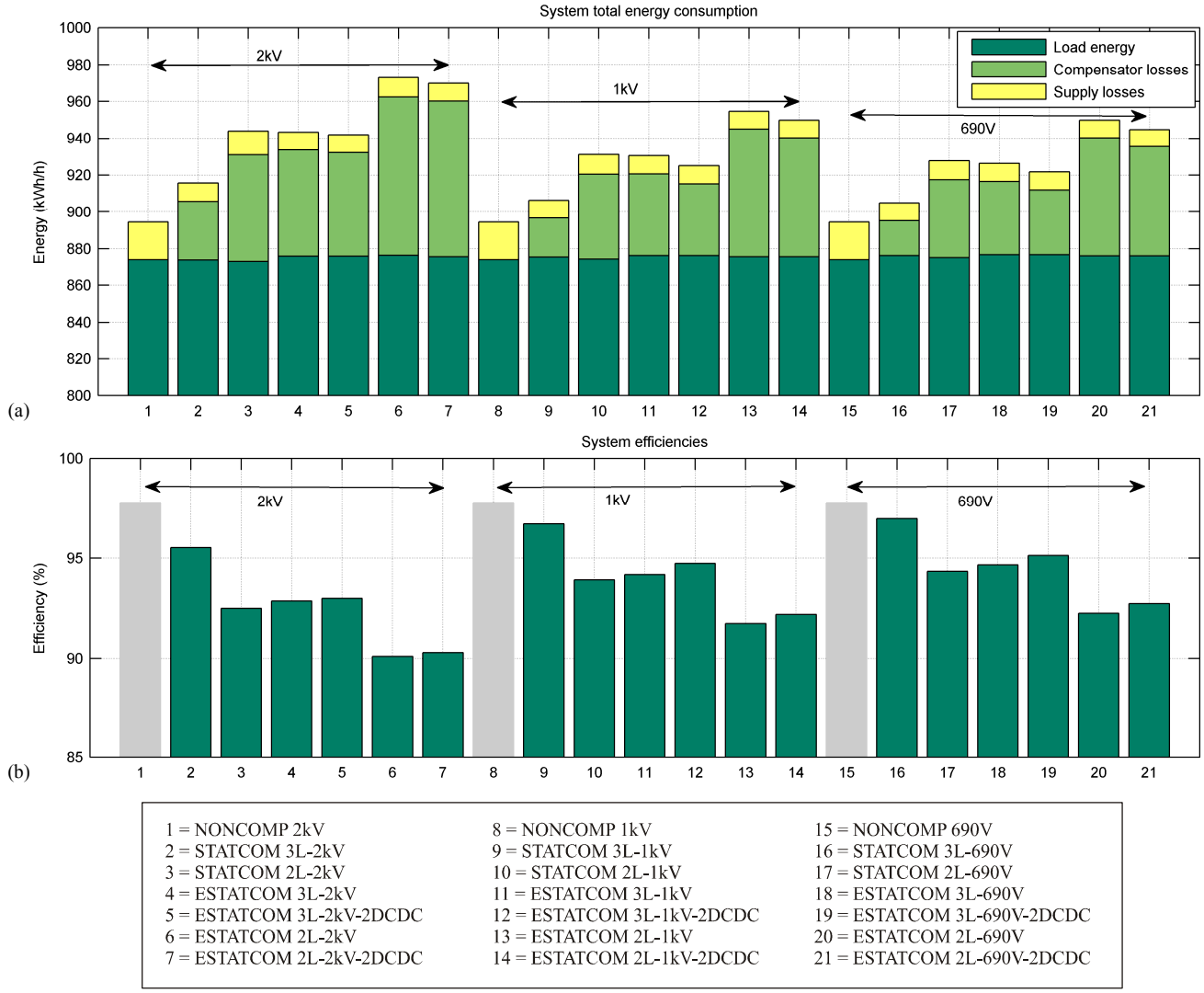

Figure 5. System (a) total energy consumptions, (b) efficiencies.

The RMS value of the current over the simulation period is 42.3 A, which depicts that the number of SC modules could be reduced to 1/3 by still maintaining the long-term current below the maximum continuous rating.

The total energy consumptions in Fig. 5a have been calculated assuming that the systems would be in operation for one hour. The efficiencies in Fig. 5b have been calculated from

$$\text{Efficiency} = \frac{\text{Load energy}}{\text{Total energy}} \cdot 100\% \cdot \qquad (1)$$

According to Fig. 5b the best efficiencies would be achieved with the NC systems. In the following analysis the NC system efficiencies have been considered as irrelevant, since the NC system causes such severe disturbations to the supply grid (Fig. 4 and Table IV), that the power system owner would prohibit the use of an EAF without any compensating device.

The lowering of the network voltage from 2 kV to 1 kV or 690 V reduces the total losses of the systems and hence increases the efficiencies. This is mainly due to the use of IGBTs with lower rated voltage within the VSCs and DC/DC converters, which produce significantly lower switching losses than those with higher voltage rating [9]. The same reason causes the systems with the 3-level VSCs to produce lower losses than the systems with the 2-level VSCs [9]. In addition, the losses caused by two separate DC/DC converters are somewhat lower than the losses of a single converter [9]. Overall, the lowest energy consumptions and best efficiencies are achieved with the systems using 3-level VSCs connected to the 690 V network, and with the use of two separate 0.55 MW DC/DC converters instead of a single 1.1 MW converter.

IV. CONCLUSION

The performances of conventional STATCOMs and STATCOMs with energy storage were analyzed in 2.1 MVA EAF applications. The analysis was done by computer simulations with Matlab Simulink software. The results show

that load compensation reduces the required current rating of the supply grid cables and transformers by approximately 30 %, and the maximum RP voltage drop is reduced to about 2 % compared to 15 % caused by the non-compensated system. The conventional STATCOM attenuates the RP voltage flicker index with a factor of 5.9 and the ESTATCOM with a factor of 11.7. The VSC bridges of both compensators could be designed for the same rated current, despite of real current compensation. The system losses are minimized when a 3-level VSC bridge is used, the STATCOM device is connected to the network voltage of 690 V, and when the ES is connected to the dc link with two separate DC/DC converters. This is mainly due to the minimized switching losses in the system converters.

REFERENCES

[1] P. Wang, N. Jenkins, M. H. J. Bollen, "Experimental investigation of voltage sag mitigation by an advanced static VAr compensator," *IEEE Transactions on Power Delivery*, vol. 13, no. 4, pp. 1461-1467, Oct. 1998.

[2] M. Routimo, A. Mäkinen, M. Salo, R. Seesvuori, J. Kiviranta, H. Tuusa, "Flicker mitigation with a hybrid compensator," *IEEE Transactions on Industry Applications*, vol. 44, no. 4, pp. 1227-1238, Jul./Aug. 2008.

[3] G.F. Reed, M. Takeda, F. Ojima, A. P. Sidell, R. E. Chervus, C. K. Nebecker, "Application of a 5 MVA, 4.16 kV D-STATCOM system for voltage flicker compensation at Seattle Iron and Metals," in *IEEE 2000 Power Engineering Society Summer Meeting*, 2000, vol. 3, pp. 1605-1611.

[4] J. Sun, D. Czarkowski, Z. Zabar, "Voltage flicker mitigation using PWM-based distribution STATCOM," in *IEEE 2002 Power Engineering Society Summer Meeting*, 2002, vol. 1, pp. 616-621.

[5] Y. Xu, L. M. Tolbert, J. D. Kueck, D. T. Rizy, "Voltage and current unbalance compensation using a static var compensator," *IET Power Electronics*, vol. 3, no. 6, pp. 977-988, Nov. 2010.

[6] A. Arulampalam, J. B. Ekanayake, N. Jenkins, "Application study of a STATCOM with energy storage," *IEE Proceedings: Generation, Transmission and Distribution*, vol. 150, no. 3, pp. 373-384, May 2003.

[7] H. Xie, L. Ängquist, H.-P. Nee, "Investigation of StatComs with capacitive energy storage for reduction of voltage phase jumps in weak networks," *IEEE Transactions on Power Systems*, vol. 24, no. 1, pp. 217-225, Feb. 2009.

[8] A. Virtanen, H. Haapala, S. Hännikäinen, T. Muhonen, H. Tuusa, "Calorimetric efficiency measurements of supercapacitors and lithium-ion batteries," in *IEEE 2011 Applied Power Electronics Conference*, 2011, pp. 1367-1373.

[9] A. Virtanen, J. Jokipii, J. Rekola, H. Tuusa, "Influence of network voltage level, converter topology and integration of energy storage on the power losses of STATCOM devices," unpublished, to be published in *IEEE 2013 Applied Power Electronics Conference*, 2013.

[10] D. G. Holmes, T. A. Lipo, *Pulse width modulation for power converters: principles and practice*, IEEE Press, Piscataway, New Jersey, USA, 2003, 724 p.

[11] A. Nabae, I. Takahashi, H. Akagi, "A new neutral-point-clamped PWM inverter," *IEEE Transactions on Industry Applications*, vol. IA-17, no. 5, pp. 518-523, Sept./Oct. 1981.

[12] J. Zhang, J.-S. Lai, R.-Y. Kim, W. Yu, "High-power density design of a soft-switching high-power bidirectional dc–dc converter," *IEEE Transactions on Power Electronics*, vol. 22, no. 4, pp. 1145-1153, Jul. 2007.

[13] R. Teodorescu, M. Liserre, P. Rodriguez, *Grid converters for photovoltaic and wind power systems*, John Wiley & Sons, West Sussex, United Kingdom, 2011, 398 p.

[14] P. Rodriguez, A. Luna, R. S. Munoz-Aguilar, I. Etxeberria-Otadui, R. Teodorescu, F. Blaabjerg, "A stationary reference frame grid synchronization system for three-phase grid-connected power converters under adverse conditions", *IEEE Transactions on Power Electronics*, vol. 27, no. 1, pp. 99–112, Jan. 2012.

[15] IEC-61000-4-15, Testing and measurement techniques – Flickermeter – Functional and design specifications, 2003, 47 p.